Somatic inactivation of E-cadherin and p53 in mice leads to metastatic lobular mammary carcinoma through induction of anoikis resistance and angiogenesis

Patrick W.B. Derksen,[1] Xiaoling Liu,[1] Francis Saridin,[1] Hanneke van der Gulden,[1] John Zevenhoven,[2] Bastiaan Evers,[1] Judy R. van Beijnum,[5] Arjan W. Griffioen,[5] Jacqueline Vink,[2] Paul Krimpenfort,[2] Johannes L. Peterse,[3] Robert D. Cardiff,[4] Anton Berns,[2] and Jos Jonkers[1,*]

[1] Division of Molecular Biology, Netherlands Cancer Institute, 1066 CX Amsterdam, The Netherlands
[2] Division of Molecular Genetics, Netherlands Cancer Institute, 1066 CX Amsterdam, The Netherlands
[3] Department of Pathology, Netherlands Cancer Institute, 1066 CX Amsterdam, The Netherlands
[4] University of California Davis Center for Comparative Medicine, Davis, California 95616
[5] Angiogenesis Laboratory, Research Institute for Growth and Development, Department of Pathology, Maastricht University, 6202 AZ Maastricht, The Netherlands
*Correspondence: j.jonkers@nki.nl

Summary

Metastatic disease is the primary cause of death in breast cancer, the most common malignancy in Western women. Loss of E-cadherin is associated with tumor metastasis, as well as with invasive lobular carcinoma (ILC), which accounts for 10%–15% of all breast cancers. To study the role of E-cadherin in breast oncogenesis, we have introduced conditional E-cadherin mutations into a mouse tumor model based on epithelium-specific knockout of p53. Combined loss of E-cadherin and p53 resulted in accelerated development of invasive and metastatic mammary carcinomas, which show strong resemblance to human ILC. Moreover, loss of E-cadherin induced anoikis resistance and facilitated angiogenesis, thus promoting metastatic disease. Our results suggest that loss of E-cadherin contributes to both mammary tumor initiation and metastasis.

Introduction

Breast cancer is the most common malignancy among females in the Western world, affecting 12% of the female population and resulting in approximately half a million deaths annually (Althuis et al., 2005). Invasive lobular carcinoma (ILC), which represents 10%–15% of all breast cancers, has a greater tendency for multifocality and bilaterality than other primary breast tumors (Arpino et al., 2004). In its classical form, ILC consists of noncohesive cells that invade the parenchyma diffusely or arranged in trabecules without mass formation, often resulting in a false-negative diagnosis using physical examination or mammography (Simpson et al., 2003).

Breast cancer progression depends on the capacity to invade and to metastasize to distant sites. Loss of tumor cell adhesion is an important factor in this process. E-cadherin is a key component of adherens junctions, structures that play crucial roles in the maintenance of epithelial integrity (Perez-Moreno et al., 2003). E-cadherin is a calcium-dependent cell adhesion molecule that mediates homophilic interactions and controls the formation of catenin-containing complexes that link E-cadherin to the actin and microtubule cytoskeleton (Hulsken et al., 1994; Takeichi, 1995; Perez-Moreno et al., 2003). In cancer, loss of E-cadherin function through genetic or epigenetic mechanisms has been implicated in progression and metastasis of numerous malignancies (Vleminckx et al., 1991; Frixen et al., 1991; Oda et al., 1994; Cleton-Jansen et al., 1994; Berx et al., 1995; Graff et al., 1995; Yoshiura et al., 1995; Savagner et al., 1997; Perl et al., 1998; Batlle et al., 2000; Cano et al., 2000; Comijn et al., 2001; Fujita et al., 2003; Yang et al., 2004; Moody et al., 2005). In breast cancer, the vast majority of ILCs have lost expression of E-cadherin, whereas most other subtypes have retained expression (Berx et al., 1995; Lehr et al., 2000; Korkola et al., 2003; Zhao et al., 2004). While metastasis to lung, liver, and bone marrow is common in most types of human breast cancer, including ILC, gastrointestinal and peritoneal metastases are more frequent in ILC (Arpino et al., 2004).

Although the expression and mutational status of E-cadherin may serve as a prognostic indicator in breast pathology, its contribution to tumor initiation, progression, and metastasis is

SIGNIFICANCE

Human invasive lobular carcinoma (ILC) is the second most common type of primary breast cancer. ILC is often difficult to diagnose and shows overall poor responses to conventional chemotherapy. This study shows that tissue-specific loss of E-cadherin and p53 in mice induces metastatic mammary carcinomas that resemble human ILC. The mouse model presented here provides a valuable tool to gain insights into the role of E-cadherin loss of function in mammary tumor initiation, progression, and metastasis and may ultimately contribute to the development of therapies for the treatment of lobular breast cancer.

largely undefined. We therefore sought to study the consequences of somatic loss of E-cadherin in a mouse mammary tumor model based on epithelium-specific inactivation of p53. The data presented here show that combined loss of E-cadherin and p53 in mammary epithelial cells induces metastatic carcinomas that resemble human ILC.

Results

Conditional inactivation of E-cadherin alone does not induce tumor formation

To study the effects of E-cadherin loss on skin and mammary tumorigenesis, we employed conditional E-cadherin (*Cdh1*) gene inactivation using the Cre/*loxP* site-specific recombination system (Figures S1A–S1C in the Supplemental Data available with this article online) and crossed the resulting $Cdh1^{F}$ conditional animals with *K14cre* transgenic mice (Figure S1D), which express the Cre recombinase in several epithelial tissues, including skin and mammary epithelium (Jonkers et al., 2001). In line with the low and stochastic *K14cre* recombinase activity in mammary epithelium (Jonkers et al., 2001), no abnormal ductal and alveolar development was observed in virgin, pregnant, or parous *K14cre;*$Cdh1^{F/F}$ mice, and dams were able to nurse their litters (data not shown). *K14cre*-mediated loss of E-cadherin alone does not predispose to cancer, as none of the *K14cre;*$Cdh1^{F/F}$ animals developed skin or mammary tumors. These findings are consistent with previous work showing that conditional inactivation of E-cadherin in either skin or mammary epithelium does not induce tumor formation (Boussadia et al., 2002; Young et al., 2003; Tinkle et al., 2004; Tunggal et al., 2005).

E-cadherin loss collaborates with p53 loss in skin and mammary tumorigenesis

To study the effects of E-cadherin loss on mammary tumor initiation, progression, and metastasis, we made use of the *K14cre;*$Trp53^{F/F}$ mouse tumor model, which gives rise to mammary carcinomas and carcinosarcomas with a median latency of 330 days (X.L., H. Holstege, H.v.d.G., M. Treur, J.Z., A. Velds, R.M. Kerkhoven, M. van Vliet, L.F.A. Wessels, J.L.P., A.B., and J.J., unpublished data). Furthermore, squamous cell carcinomas of the skin developed in approximately 25% of the *K14cre;*$Trp53^{F/F}$ females. As most carcinomas in *K14cre;*$Trp53^{F/F}$ animals are nonmetastatic, this model is suitable for investigating phenotypic consequences of additional mutations in genes implicated in tumor progression and metastasis. We therefore introduced the $Cdh1^{F}$ allele into the *K14cre;*$Trp53^{F/F}$ model to produce *K14cre;*$Cdh1^{F/F}$;$Trp53^{F/F}$, *K14cre;*$Cdh1^{F/+}$;$Trp53^{F/F}$, and *K14cre;*$Cdh1^{F/F}$;$Trp53^{F/+}$ females, which were monitored for spontaneous tumor development and progression. Homozygous mutation of E-cadherin resulted in accelerated development of skin and mammary tumors in *K14cre;*$Cdh1^{F/F}$;$Trp53^{F/F}$ female mice, compared to the *K14cre;*$Trp53^{F/F}$ females ($p < 0.0001$; Figure 1A, left panels, and Figure S2), demonstrating that E-cadherin loss of function collaborates with p53 inactivation in epithelial tumorigenesis. *K14cre;*$Cdh1^{F/F}$;$Trp53^{F/F}$ mice developed multiple skin and mammary tumors with a median latency of 214 days. In contrast, *K14cre;*$Trp53^{F/F}$ females developed mostly single mammary tumors and small numbers of skin carcinomas with a median latency of 330 days. We observed significantly longer tumor latency periods for *K14cre;*$Cdh1^{F/+}$;$Trp53^{F/F}$ and *K14cre;*$Cdh1^{F/F}$;$Trp53^{F/+}$ females (330 and 495 days, respectively; $p < 0.0001$; Figure 1A, upper right and lower left panels, and Figure S2), showing that E-cadherin and p53 loss of function effectively synergize in skin and mammary tumorigenesis.

We next determined the genetic status of *Cdh1* and *Trp53* in the panels of mammary tumors derived from the different compound mutant mouse strains. Southern blot analysis showed stochastic loss of the conditional *Cdh1* allele in tumors derived from *K14cre;*$Cdh1^{F/+}$;$Trp53^{F/F}$ animals, whereas the wild-type *Cdh1* allele was retained (Figure 1B). Because the tumor-free survival curves for the *K14cre;*$Cdh1^{F/+}$;$Trp53^{F/F}$ and *K14cre;*$Trp53^{F/F}$ females were identical (Figure 1A, lower right panel), we conclude that E-cadherin is not haploinsufficient for tumor suppression. In contrast to the stochastic loss of the conditional *Cdh1* allele in *K14cre;*$Cdh1^{F/+}$;$Trp53^{F/F}$ mammary tumors, we detected uniform loss of both conditional *Cdh1* alleles in the majority of mammary tumors from *K14cre;*$Cdh1^{F/F}$;$Trp53^{F/+}$ and *K14cre;*$Cdh1^{F/F}$;$Trp53^{F/F}$ females (Figure 1B). We also detected loss of the conditional and wild-type *Trp53* alleles in all mammary tumors from *K14cre;*$Cdh1^{F/+}$;$Trp53^{F/F}$, *K14cre;*$Cdh1^{F/F}$;$Trp53^{F/+}$, and *K14cre;*$Cdh1^{F/F}$;$Trp53^{F/F}$ females (Figure 1B), indicating that, in these mice, loss of functional p53 is a prerequisite for mammary tumor formation.

Loss of E-cadherin and p53 induces invasive skin carcinoma

Skin tumors from *K14cre;*$Trp53^{F/F}$ or *K14cre;*$Cdh1^{F/+}$;$Trp53^{F/F}$ mice could be classified as either pilomatricomas or squamous cell carcinomas with expansive growth patterns without evident metastasis (Figure S3, left panels). In contrast, homozygous mutation of E-cadherin in *K14cre;*$Cdh1^{F/F}$;$Trp53^{F/F}$ and *K14cre;*$Cdh1^{F/F}$;$Trp53^{F/+}$ animals had a dramatic impact on skin tumor phenotype. Skin tumors from these animals often showed a phenotypic change from expansive to invasive growth (Figure S3, right panels). Tumors invaded subcutaneous fat and carnosus muscle in irregular strands and nest with polymorphic cells with dyskeratosis (Figure S3, right panels). Tumor cells expressed cytokeratin 14 (CK14) (Figures S3C and S3D) but lacked expression of CK1 and CK6 (data not shown), suggesting a basal origin. Occasionally, draining lymph nodes contained malignant epithelial cells, but distant metastases were absent.

Loss of E-cadherin induces a shift from expansive carcinoma to invasive lobular carcinoma

Most mammary tumors from *K14cre;*$Trp53^{F/F}$ or *K14cre;*$Cdh1^{F/+}$;$Trp53^{F/F}$ females were diagnosed as intermediate-grade adenocarcinomas or high-grade solid carcinomas, characterized by an expansive growth pattern and consisting of large epithelial cells forming solid nests or irregular glands (X.L., H. Holstege, H.v.d.G., M. Treur, J.Z., A. Velds, R.M. Kerkhoven, M. van Vliet, L.F.A. Wessels, J.L.P., A.B., and J.J., unpublished data, and Figure 2, left panels). Adenocarcinomas and solid carcinomas uniformly expressed CK8 and showed occasional sporadic expression of CK14 but lacked expression of vimentin (Figure 2, left panels; Table S1) and smooth muscle actin (SMA; data not shown). The third most common tumor type shows a carcinosarcoma phenotype, characterized by a metaplastic and biphasic histology comprised of epithelial and mesenchymal elements. These tumors show a heterogeneous expression pattern for CK8 and 14, often express vimentin, and mostly lack expression of E-cadherin (Table S1). Adenocarcinomas and solid carcinomas

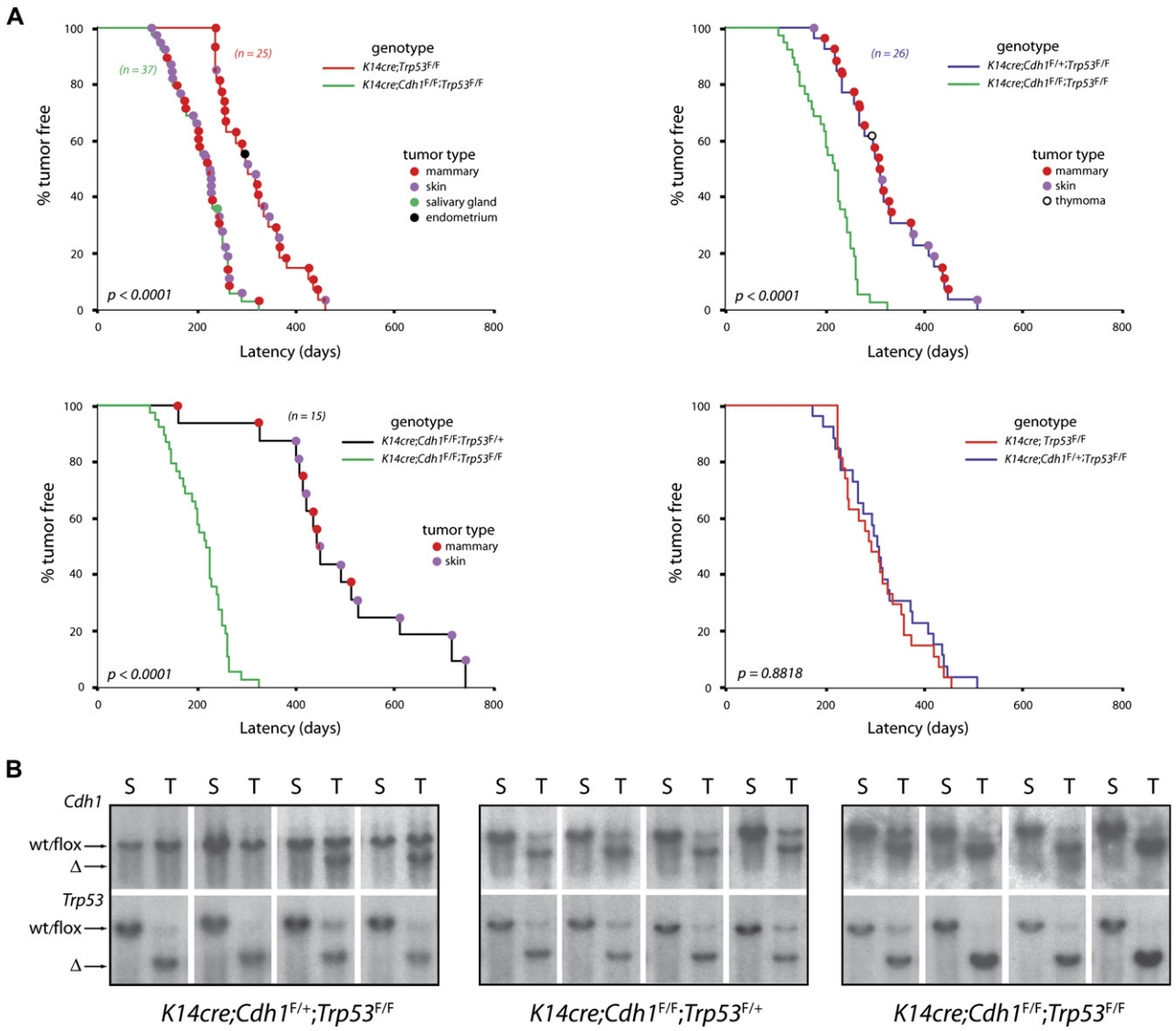

Figure 1. Synergistic tumor suppressor activity of E-cadherin and p53

A: Tumor incidence and spectrum of tumors in *K14cre* females carrying conditional alleles for *Cdh1* and *Trp53*. Kaplan-Meier tumor-free survival curves for *K14cre;Cdh1*$^{F/F}$*;Trp53*$^{F/F}$ versus *K14cre;Trp53*$^{F/F}$ (upper left panel), *K14cre;Cdh1*$^{F/+}$*;Trp53*$^{F/F}$ (upper right panel), and *K14cre;Cdh1*$^{F/F}$*;Trp53*$^{F/+}$ (lower left panel) females. Tumor types for each animal are indicated in colored bullets. Lower right panel shows a tumor-free survival curve of *K14cre;Cdh1*$^{F/+}$*;Trp53*$^{F/F}$ versus *K14cre;Trp53*$^{F/F}$ females illustrating that heterozygosity of *Cdh1* does not accelerate tumor formation. Mice were killed when tumors reached an average diameter of 10 mm (mammary tumors) or 7 mm (skin tumors). Mammary tumor size was used as the primary criterion.

B: *Cdh1* and *Trp53* inactivation in mammary tumors. Southern blot analysis of tumor DNA to detect Cre-mediated inactivation of *Cdh1* (ScaI digestion, exon 16 probe) and *Trp53* (BglII digestion, exon 11 probe). Shown are representative tumors (T) and control spleens (S) from the same animal. wt/flox, wild-type or conditional allele. Δ, switched allele.

from *K14cre;Trp53*$^{F/F}$ and *K14cre;Cdh1*$^{F/+}$*;Trp53*$^{F/F}$ females expressed E-cadherin and showed expansive, rather than invasive growth (Figure 2, left panels, and Table S1).

Somatic loss of E-cadherin in *K14cre;Cdh1*$^{F/F}$*;Trp53*$^{F/F}$ and *K14cre;Cdh1*$^{F/F}$*;Trp53*$^{F/+}$ females resulted in a significant shift from expansive to invasive carcinoma ($p < 0.01$; Table 1), which showed strong phenotypic similarities to human ILC (Figure 2, middle and right panels). These tumors, which we designate mouse invasive lobular carcinoma (mILC), developed with high incidence multifocally in several mammary glands ($p < 0.0001$; Table 1). mILC cells were small in size and uniform in appearance. Like the adenocarcinomas and solid carcinomas from the *K14cre;Cdh1*$^{F/+}$*;Trp53*$^{F/F}$ females, lobular carcinomas from *K14cre;Cdh1*$^{F/F}$*;Trp53*$^{F/F}$ and *K14cre;Cdh1*$^{F/F}$*;Trp53*$^{F/+}$ females expressed CK8 and occasionally expressed CK14, but did not express vimentin (Figure 2, middle panels and Table S1) or SMA (data not shown), indicating that mILC cells have epithelial properties. mILCs from *K14cre;Cdh1*$^{F/F}$*;Trp53*$^{F/F}$ and *K14cre;Cdh1*$^{F/F}$*;Trp53*$^{F/+}$ females were estrogen receptor (ER) negative and showed no overexpression of *Erbb2* mRNA or amplification of the *Erbb2* gene (data not shown). Also, carcinosarcomas were found in *K14cre;Cdh1*$^{F/F}$*;Trp53*$^{F/F}$ and *K14cre;Cdh1*$^{F/F}$*;Trp53*$^{F/+}$ females. While displaying mILC components, these tumors predominantly exhibited a spindle-shaped cell morphology, presenting large cells with pleomorphic nuclei, coarsely clumped chromatin, and sparse cytoplasm.

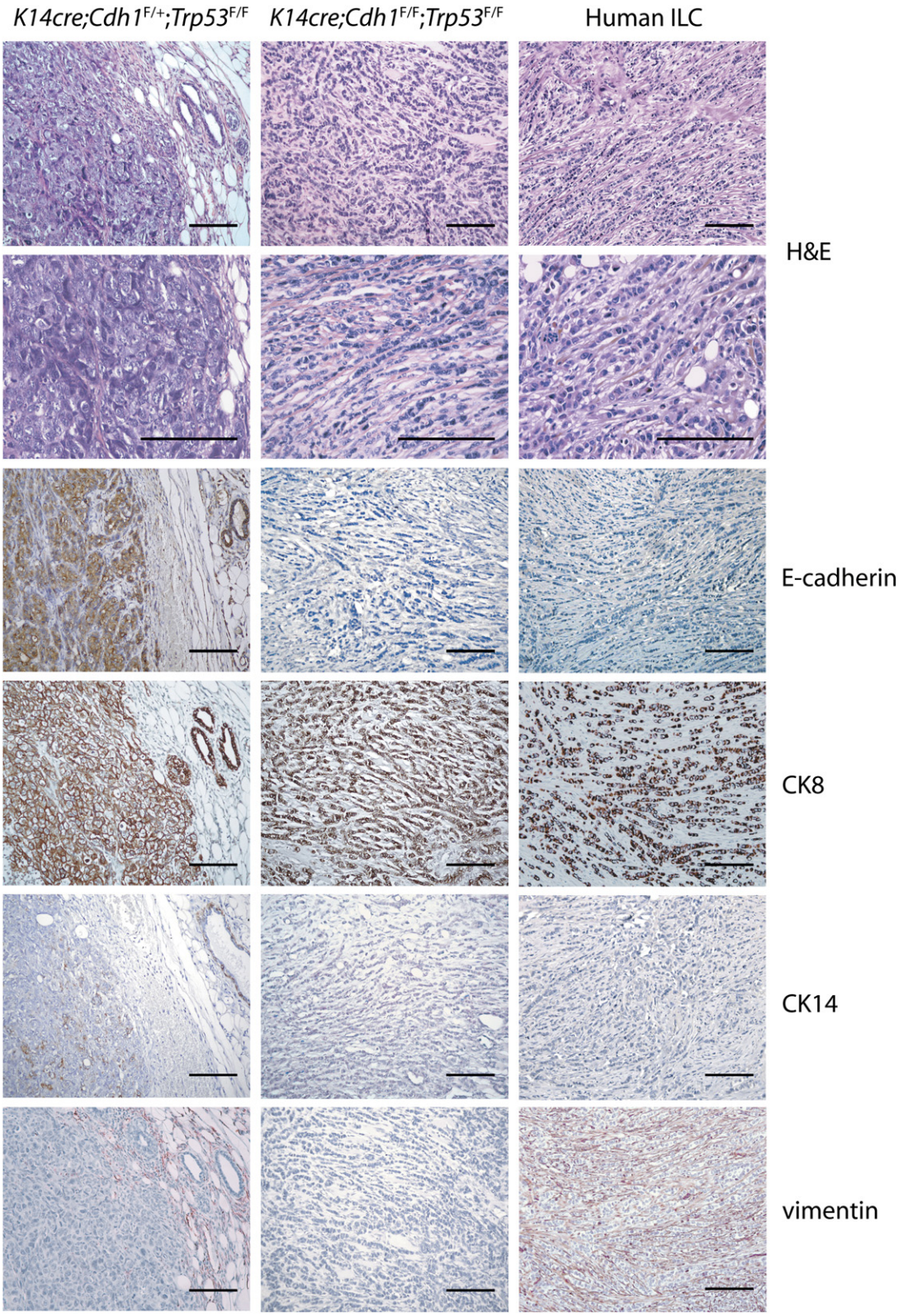

Figure 2. Conditional inactivation of E-cadherin and p53 in mammary epithelium induces mouse invasive lobular carcinoma

Histopathology of mammary tumors derived from *K14cre;Cdh1$^{F/+}$;Trp53$^{F/F}$* (left panels) and *K14cre;Cdh1$^{F/F}$;Trp53$^{F/F}$* (middle panels) female mice and a human patient diagnosed with invasive lobular carcinoma (ILC) (right panels). Left panels show an adenocarcinoma derived from a *K14cre;Cdh1$^{F/+}$;Trp53$^{F/F}$* female. Middle panels show the consequence of homozygous inactivation of E-cadherin in mammary tumors from *K14cre;Cdh1$^{F/F}$;Trp53$^{F/F}$* females. Tumors have undergone a switch from an expansive to an invasive carcinoma resembling human ILC. mILCs are characterized by a trabecular or ''single file'' arrangement of cells, are poorly differentiated, and are small in size and uniform in nuclear and cytoplasm. Tumor cells show invasive characteristics, infiltrating abundantly present fibrous stromal tissues. The bottom H&E stainings show enlargements of the top panels. Scale bars, 100 μm.

Table 1. Somatic inactivation of E-cadherin leads to invasive and metastatic mILC in the *K14cre;Cdh1^{F};Trp53^{F}* mouse model

	K14cre;Cdh1$^{F/+}$; Trp53$^{F/F}$	*K14cre;Cdh1$^{F/F}$; Trp53$^{F/F}$*	χ^2 p value
Invasive growth*	4/19 (21%)	14/21 (67%)	<0.01
Metastasis*	3/19 (16%)	10/21 (48%)	<0.05
Adenocarcinoma, solid carcinoma	13/19 (68%)	5/22 (23%)	<0.01
Carcinosarcoma	10/19 (53%)	6/22 (27%)	0.120
mILC	0/19 (0%)	12/22 (54%)	<0.0001

*Significance of growth patterns (invasive versus expansive) and metastasis were calculated for the carcinomas only. Statistical significance (p values) was determined using a Pearson exact χ^2 test (two-sided).

Spindle-shaped tumor cells showed both expansive and invasive growth patterns, heterogeneously expressed CK8 and CK14, and mostly expressed vimentin, but lacked expression of E-cadherin and SMA (Table S1 and data not shown).

Loss of E-cadherin contributes to mammary tumor initiation

Cre recombinase activity in mammary epithelium of *K14cre* transgenic females is relatively low, thus resulting in stochastic recombination of varying numbers of recombined alleles in individual Cre-expressing mammary epithelial cells (Jonkers et al., 2001). The low activity of K14cre in mammary epithelium is exemplified by the mammary tumors from *K14cre;Cdh1$^{F/+}$; Trp53$^{F/F}$* females, which show—in addition to uniform recombination of both conditional *Trp53* alleles—stochastic recombination of the single conditional *Cdh1* allele (Figure 1B). Hence, the fact that the vast majority of primary mammary tumors from *K14cre;Cdh1$^{F/F}$;Trp53$^{F/F}$* females have lost E-cadherin indicates selection for E-cadherin mutation during primary tumor formation, suggesting that E-cadherin loss of function contributes to tumor initiation. To verify this, we analyzed macroscopically tumor-free mammary glands from *K14cre;Cdh1$^{F/F}$; Trp53$^{F/F}$* female animals for ductal morphology and E-cadherin expression. Immunohistochemical staining showed that E-cadherin expression was maintained in normal mammary epithelium of *K14cre;Cdh1$^{F/F}$;Trp53$^{F/F}$* females. However, ducts could be found partly lined by or filled by atypical cells with luminal characteristics that lacked expression of E-cadherin and showed increased proliferation (Figure 3), suggesting that these cells represent an early, noninvasive (in situ) stage of tumor development. These findings indicate that loss of E-cadherin not only promotes mammary tumor progression and metastasis, but also contributes to tumor initiation in *K14cre;Cdh1^{F};Trp53^{F}* females.

Loss of E-cadherin induces metastatic mILC

To explore whether mILC mimics the metastatic pattern of human ILC, we performed a detailed histological survey into the metastatic spread of mILC. From the *K14cre;Cdh1$^{F/F}$;Trp53$^{F/F}$* and *K14cre;Cdh1$^{F/F}$;Trp53$^{F/+}$* females that presented carcinomas of approximately 1 cm in diameter, 14 out of 21 showed extensive local invasion ($p < 0.01$; Table 1), and 10 out of 21 showed metastases to draining and distant lymph nodes ($p < 0.05$; Table 1) (Figures 4C and 4D; Table S1). Also, in a minority of animals dissociated or loosely clustered mILC cells were detected in organs such as lungs, liver, gastrointestinal and urogenital tract, and pancreas, or diffusely disseminated throughout the peritoneal cavity (Figures 4E–4L), indicating that mILC recapitulates the histopathology and tumor biology of human ILC. All mILC metastases expressed CK8 and showed a cellular morphology similar to that of the primary tumor (Figures 4A–4L and data not shown). Moreover, we frequently observed mILC cells infiltrating desmoplastic stroma arranged in single cell rows, forming stellate lesions and occasionally showing targetoid periductal distributions, which are typical features of human ILC (Figures 4M–4P). In contrast to the frequent occurrence of metastasis in *K14cre;Cdh1$^{F/F}$;Trp53$^{F/F}$* and *K14cre;Cdh1$^{F/F}$;Trp53$^{F/+}$* females, metastasis was only sporadically observed in *K14cre;Cdh1$^{F/+}$;Trp53$^{F/F}$* females (Table 1 and Figure S1). Three *K14cre;Cdh1$^{F/+}$;Trp53$^{F/F}$* females with a mixed carcinosarcoma/carcinoma tumor morphology showed dissemination of tumor cells to regional lymph nodes or lungs. Interestingly, one of these tumors had lost expression of E-cadherin (Table S1).

To investigate the pattern of mILC metastasis in more detail, we isolated primary mammary tumor cells from *K14cre;Trp53$^{F/F}$*

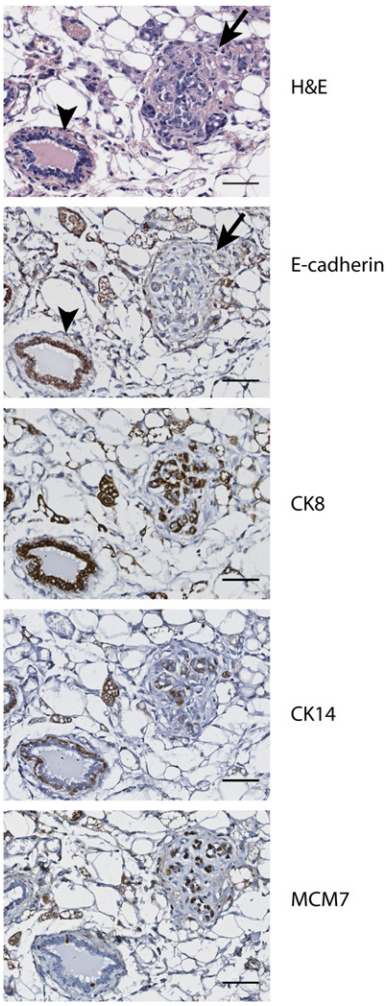

Figure 3. Loss of E-cadherin is an early event in mammary tumor formation
Histopathology of serial sections from a *K14cre;Cdh1$^{F/F}$;Trp53$^{F/F}$* female mice, showing early in situ lesions lacking E-cadherin (arrow) expression. Arrowhead indicates a normal mammary duct. MCM7, Cdc47 proliferation marker. Scale bars, 100 μm.

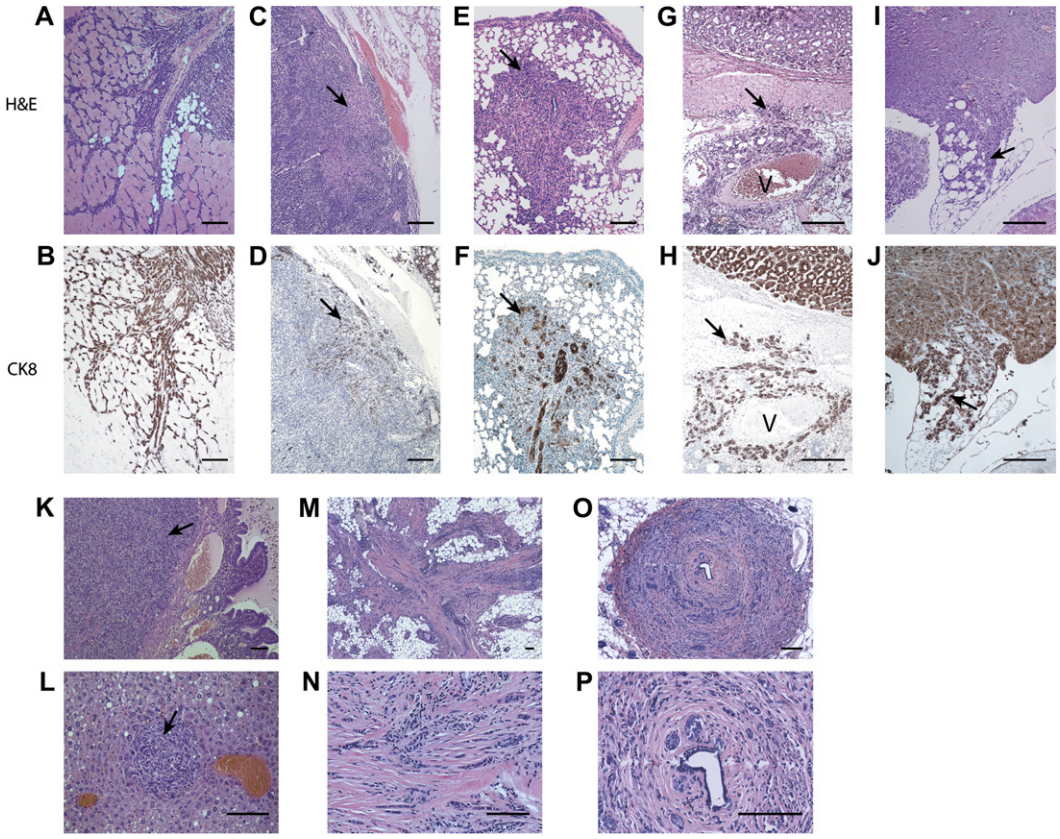

Figure 4. mILC resembles the invasive and metastatic characteristics of human ILC

A and B: Infiltration of the striated muscle of the hind limb by mILC cells, which originate from a primary tumor present in the adjacent fifth mammary gland. **C–F:** Distant metastasis of mILC. Carcinoma cells are infiltrating the medullary sinus of the axillary lymph node (arrow) (**C** and **D**) and lungs (**E** and **F**). **G and H:** Gastric involvement in mILC. Sections showing extravasation of mILC cells from the vena gastrica, invading into the muscularis externa of the stomach (arrow). Note the expression of CK8 on the invading ILC cells. V, vein. **I and J:** Peritoneal metastasis of mILC. Sections showing mILC metastasis to pancreas. **K and L:** Sections showing metastasis of mILC to bladder and liver, respectively. **M–P:** mILC displays characteristic features of human ILC. **M and N:** Stellate lesions in mILC. mILC cells infiltrating desmoplastic stroma arranged in single cell rows. **N** is an enlargement of **M**. **O and P:** Targetoid periductal distributions in mILC, with periductal infiltration of mILC cells surrounding a normal duct. **P** is an enlargement of **O**.
Sections were stained with H&E (**A**, **C**, **E**, **G**, **I**, and **K**–**P**) or with antibody against cytokeratin 8 (**B**, **D**, **F**, **H**, and **J**). Scale bars, 100 μm.

and *K14cre;Cdh1*$^{F/F}$*;Trp53*$^{F/F}$ females, which were cultured and subsequently transduced with luciferase-encoding lentiviruses. Mice that were orthotopically transplanted with small numbers of luciferase-expressing *Cdh1*$^{\Delta/\Delta}$*;Trp53*$^{\Delta/\Delta}$ tumor cells showed distant metastases, which could be imaged using noninvasive bioluminescence imaging 5 weeks posttransplantation (Figure 5A). Metastases were detected in the peritoneal and thoracic cavity, contralateral mammary glands, and lungs (Figures 5B–5E). In addition, we detected osteolytic bone metastases in the vertebrae of the spinal column infiltrating the spinal cord (Figure 5C). These data show that the full metastatic spectrum of human ILC is recapitulated by the *K14cre;Cdh1*^{F}*;Trp53*^{F} mILC model.

In contrast to *Cdh1*$^{\Delta/\Delta}$*;Trp53*$^{\Delta/\Delta}$ tumor cells, orthotopic transplantation of luciferase-marked *Trp53*$^{\Delta/\Delta}$ tumor cells did not result in local tumor growth and metastasis. In these animals, the bioluminescence signal decreased to undetectable levels over time (Figure 5A), suggesting that orthotopically transplanted *Trp53*$^{\Delta/\Delta}$ mammary tumor cells are not able to survive in the absence of a comprehensive endogenous microenvironment.

Loss of E-cadherin induces resistance to anoikis

The difference in survival between *Trp53*$^{\Delta/\Delta}$ and *Cdh1*$^{\Delta/\Delta}$*; Trp53*$^{\Delta/\Delta}$ tumor cells in situ prompted us to investigate their in vitro survival characteristics. We therefore cultured cells on noncoated polystyrene dishes to assess detachment-induced apoptosis (anoikis). In the absence of cell-matrix interaction, E-cadherin-expressing *Trp53*$^{\Delta/\Delta}$ tumor cell lines underwent anoikis, resulting in more than 70%–80% apoptotic cells after approximately 4 days of culturing. Interestingly, *Cdh1*$^{\Delta/\Delta}$*; Trp53*$^{\Delta/\Delta}$ cells could survive and proliferate in an anchorage-independent fashion, resulting in less than 10%–30% apoptotic cells after 4 days of culture on a noncoated polystyrene surface (Figures 6A–6C). Anoikis resistance was observed for cell lines derived from four independent *Cdh1*$^{\Delta/\Delta}$*;Trp53*$^{\Delta/\Delta}$ primary tumors, whereas cultured cells from four independent *Trp53*$^{\Delta/\Delta}$ tumors showed sensitivity to anoikis ($p < 0.005$; Figure 6C), indicating that loss of E-cadherin facilitates survival of mammary tumor cells in the absence of cell-matrix interactions.

To determine whether loss of E-cadherin directly induces anchorage-independent cell survival, we tested whether

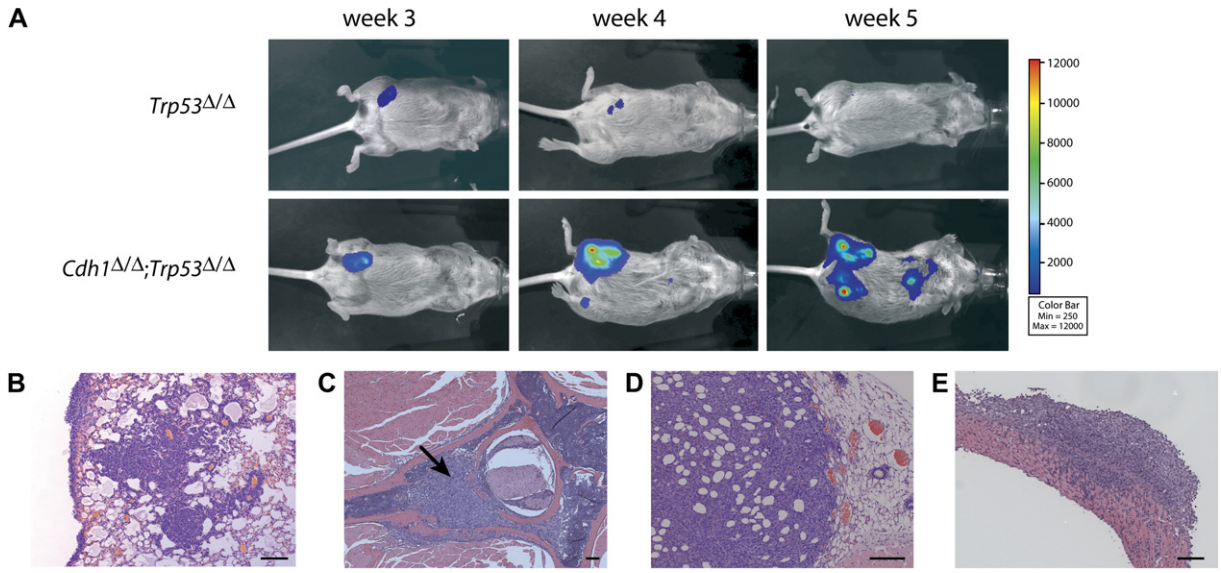

Figure 5. In vivo imaging of metastatic mILC

A: Bioluminescence imaging of recipient animals, orthotopically transplanted with luciferase-transduced mammary tumor cells derived from a *K14cre;Trp53$^{F/F}$* mouse (top panels) or *K14cre;Cdh1$^{F/F}$;Trp53$^{F/F}$* mouse (bottom panels). The color bar represents bioluminescence intensity counts. Transplantations were performed in a minimum of ten recipient animals. Results were confirmed using two independent *Trp53$^{\Delta/\Delta}$* and two different *Cdh1$^{\Delta/\Delta}$;Trp53$^{\Delta/\Delta}$* cell lines.
B–E: H&E staining of metastases to lungs (**B**), caudal vertebrae of the spinal column (arrow) (**C**), contralateral fourth mammary gland (**D**), and peritoneum, showing invasion of mILC cells into the diaphragm (**E**). Scale bars, 100 μm.

restoration of E-cadherin expression in *Cdh1$^{\Delta/\Delta}$;Trp53$^{\Delta/\Delta}$* cells would restore their capacity to undergo anoikis. After transduction of *Cdh1$^{\Delta/\Delta}$;Trp53$^{\Delta/\Delta}$* cells with ecotropic retroviruses encoding mouse E-cadherin, the majority of the E-cadherin-expressing *Cdh1$^{\Delta/\Delta}$;Trp53$^{\Delta/\Delta}$* cells underwent anoikis, while the parental *Cdh1$^{\Delta/\Delta}$;Trp53$^{\Delta/\Delta}$* cells survived (Figure 6E). These data show that E-cadherin reexpression can effectively counteract the survival phenotype of *Cdh1$^{\Delta/\Delta}$;Trp53$^{\Delta/\Delta}$* cells, suggesting that loss of E-cadherin plays a causal role in the acquisition of anoikis resistance.

Induction of angiogenesis in murine ILC

Histological analysis revealed massive central necrosis in E-cadherin-proficient mammary tumors from *K14cre;Cdh1$^{F/+}$;Trp53$^{F/F}$* females, whereas necrotic cells were rare or absent in E-cadherin-deficient tumors from *K14cre;Cdh1$^{F/F}$;Trp53$^{F/F}$* females (Figure 7A). These findings prompted us to investigate differences in vascularization between the aforementioned tumors. Staining of tumor sections with the endothelial marker CD31 showed large numbers of uniformly distributed blood vessels in mILCs from *K14cre;Cdh1$^{F/F}$;Trp53$^{F/F}$* females. In contrast, tumors harvested from *K14cre;Cdh1$^{F/+}$;Trp53$^{F/F}$* females displayed notably less vascularization, present mainly in the periphery of the tumor (Figure 7B). Quantification of the number of CD31-positive vessels in viable tumor areas of *K14cre;Cdh1$^{F/+}$;Trp53$^{F/F}$* and *K14cre;Cdh1$^{F/F}$;Trp53$^{F/F}$* carcinomas showed a 3-fold increase in vasculature in mILC ($p < 0.0001$; Figure 7C).

To verify whether mILC cells are a source of angiogenic factors, we harvested conditioned medium (CM) from *Trp53$^{\Delta/\Delta}$* and *Cdh1$^{\Delta/\Delta}$;Trp53$^{\Delta/\Delta}$* primary tumor cells cultured under serum-free conditions and performed an in vitro endothelial sprouting assay to examine induction of de novo vascularization. Indeed, CM from *Cdh1$^{\Delta/\Delta}$;Trp53$^{\Delta/\Delta}$* tumor cells induced extensive sprouting of bovine endothelial cells, whereas only marginal sprouting was observed when endothelial cells were incubated with CM from *Trp53$^{\Delta/\Delta}$* tumor cells (Figures 7D and 7E). These data suggest that E-cadherin loss of function promotes the expression of proangiogenic factors that mediate tumor vascularization in mILC.

Discussion

Loss of E-cadherin has been extensively implicated in the progression and dissemination of human cancer (Berx and van Roy, 2001; Conacci-Sorrell et al., 2002; Cavallaro and Christofori, 2004). Although a plethora of in vitro and clinical data suggest a strong involvement of E-cadherin mutation or silencing in lobular breast carcinoma, proof of a causal role for E-cadherin mutation in this malignancy is still lacking. Here, we present in vivo evidence that E-cadherin loss of function collaborates with p53 inactivation in the genesis, progression, and metastasis of mammary carcinoma. Furthermore, we impart a mouse model for human ILC, which represents up to 15% of invasive breast malignancies.

E-cadherin loss promotes both primary tumor formation and metastatic disease

Our model shows that E-cadherin acts as a tumor suppressor in the absence of p53 and that loss of E-cadherin and p53 effectively synergize in tumor formation. While combined inactivation of E-cadherin and p53 seems a prerequisite for mILC development, reduction in E-cadherin gene dosage does not provide a growth advantage in our model. Although we cannot exclude the possibility that E-cadherin has been silenced by either genetic or epigenetic mechanisms, selection for loss of the wild-type *Cdh1* allele was not a common feature in tumors from *K14cre;Cdh1$^{F/+}$;Trp53$^{F/F}$* animals. This finding was unexpected,

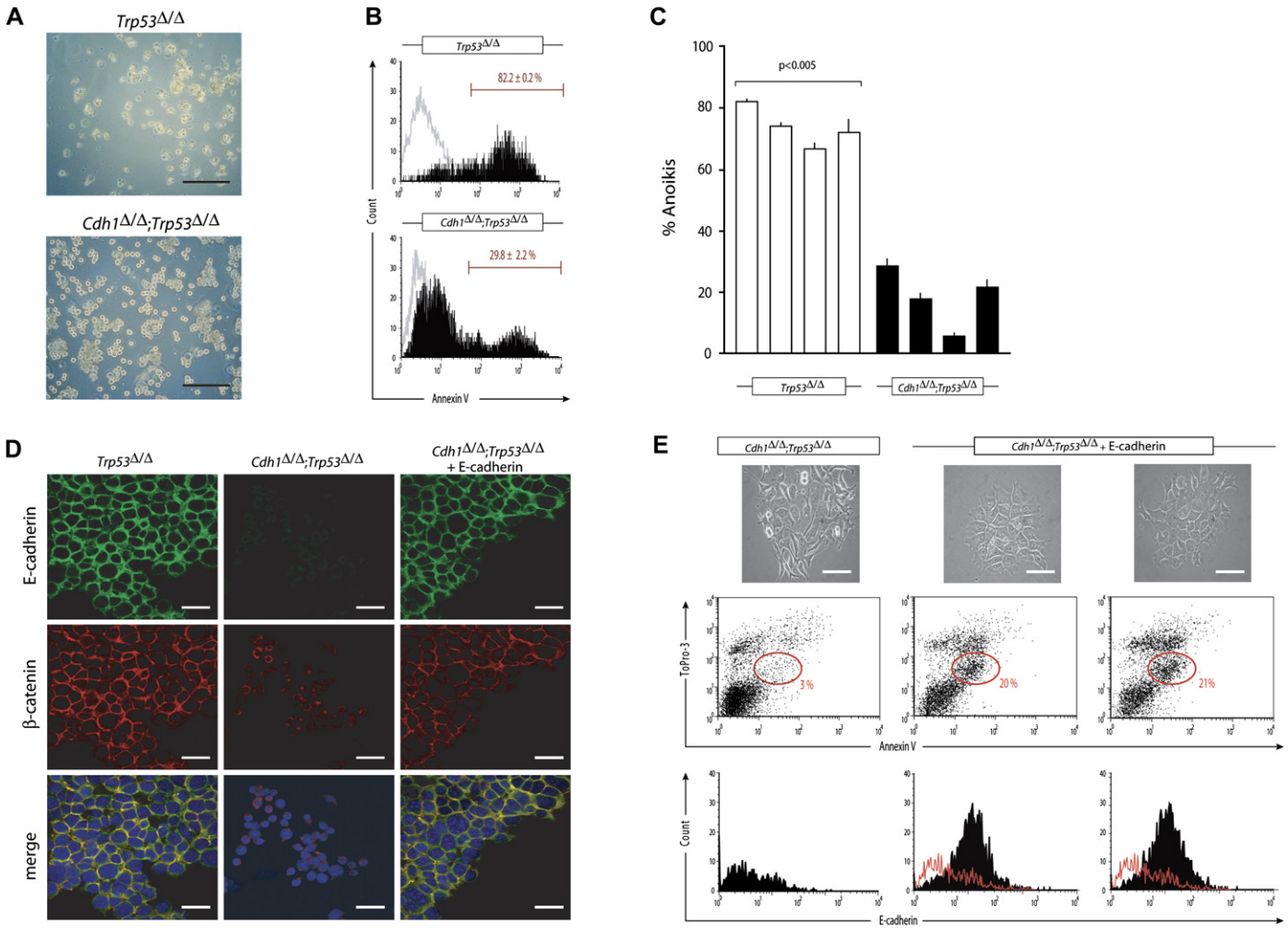

Figure 6. Loss of E-cadherin induces anoikis resistance

A: Eight primary tumor cell lines derived from independent *K14cre;Trp53$^{F/F}$* and *K14cre;Cdh1$^{F/F}$;Trp53$^{F/F}$* mammary tumors were cultured for approximately 4 days on a noncoated polystyrene surface. Scale bars, 80 μm.

B: The percentage of apoptotic tumor cells expressing phosphatidylserine was determined using binding to FITC-conjugated Annexin-V. In the presence of E-cadherin, tumor cells are not able to survive in the absence of cell-matrix interactions (top panel; *Trp53$^{\Delta/\Delta}$* cells). In contrast, mILC cells show anoikis resistance (bottom panel; *Cdh1$^{\Delta/\Delta}$;Trp53$^{\Delta/\Delta}$* cells). Gray lines represent Annexin-V binding of input material.

C: Mammary tumor cell lines derived from four independent *K14cre;Trp53$^{F/F}$* tumors (white bars) and four independent *K14cre;Cdh1$^{F/F}$;Trp53$^{F/F}$* tumors (black bars) were assayed for anoikis resistance as in **B**. Error bars represent the standard deviation of triplicate measurements.

D: Reintroduction of functional E-cadherin in *Cdh1$^{\Delta/\Delta}$;Trp53$^{\Delta/\Delta}$* cells. *Cdh1$^{\Delta/\Delta}$;Trp53$^{\Delta/\Delta}$* cells were transduced and stained for E-cadherin (top panels) and β-catenin (middle panels). Blue represents nuclear DNA staining using ToPro-3. Scale bars, 15 μm.

E: Restoration of epithelial characteristics and anoikis sensitivity upon expression of exogenous E-cadherin. *Cdh1$^{\Delta/\Delta}$;Trp53$^{\Delta/\Delta}$* cells (left panels) were transduced with E-cadherin (center and right panels). Photographs show the induction of epithelial cell morphology (center and right panels; scale bars, 20 μm). Transduced cells were then cultured for 2 days on a noncoated polystyrene surface and assayed for apoptosis (dot plots). Early apoptotic populations (encircled; Annexin-V-positive/Topro-3-negative) were gated and analyzed for E-cadherin expression (histograms). Red lines represent E-cadherin expression signal of early apoptotic *Cdh1$^{\Delta/\Delta}$;Trp53$^{\Delta/\Delta}$* cells.

considering that E-cadherin loss of function in sporadic breast cancer frequently occurs by loss of heterozygosity (LOH) (Vos et al., 1997; Berx et al., 1998) or epigenetic silencing (Cano et al., 2000; Comijn et al., 2001; Hajra et al., 2002; Yang et al., 2004). This difference may be explained by the fact that the efficiency of Cre-mediated deletion in *K14cre*-expressing mammary epithelial cells is approximately 60% per conditional allele (Jonkers et al., 2001), whereas LOH occurs with a much lower efficiency of approximately 10^{-4} per cell generation per allele (Adams and Bradley, 2002). Consequently, mammary tumorigenesis in *K14cre;Cdh1$^{F/+}$;Trp53$^{F/F}$* mice may be dominated by p53 inactivation in combination with oncogenic mutations that may occur more efficiently and/or collaborate more effectively with p53 abrogation than E-cadherin LOH. Of note, synergy between p53 abrogation and E-cadherin inactivation is clearly demonstrated by the accelerated tumor development in *K14cre;Cdh1$^{F/F}$;Trp53$^{F/F}$* mice compared to *K14cre;Cdh1$^{F/F}$* animals.

K14cre-mediated conditional inactivation of E-cadherin alone in mammary epithelium does not predispose to tumors. This is probably due to the fact that E-cadherin loss in mouse mammary epithelium is not tolerated as a result of the rapid induction of apoptosis (Boussadia et al., 2002). In concordance with this, we did not detect ductal structures lacking E-cadherin

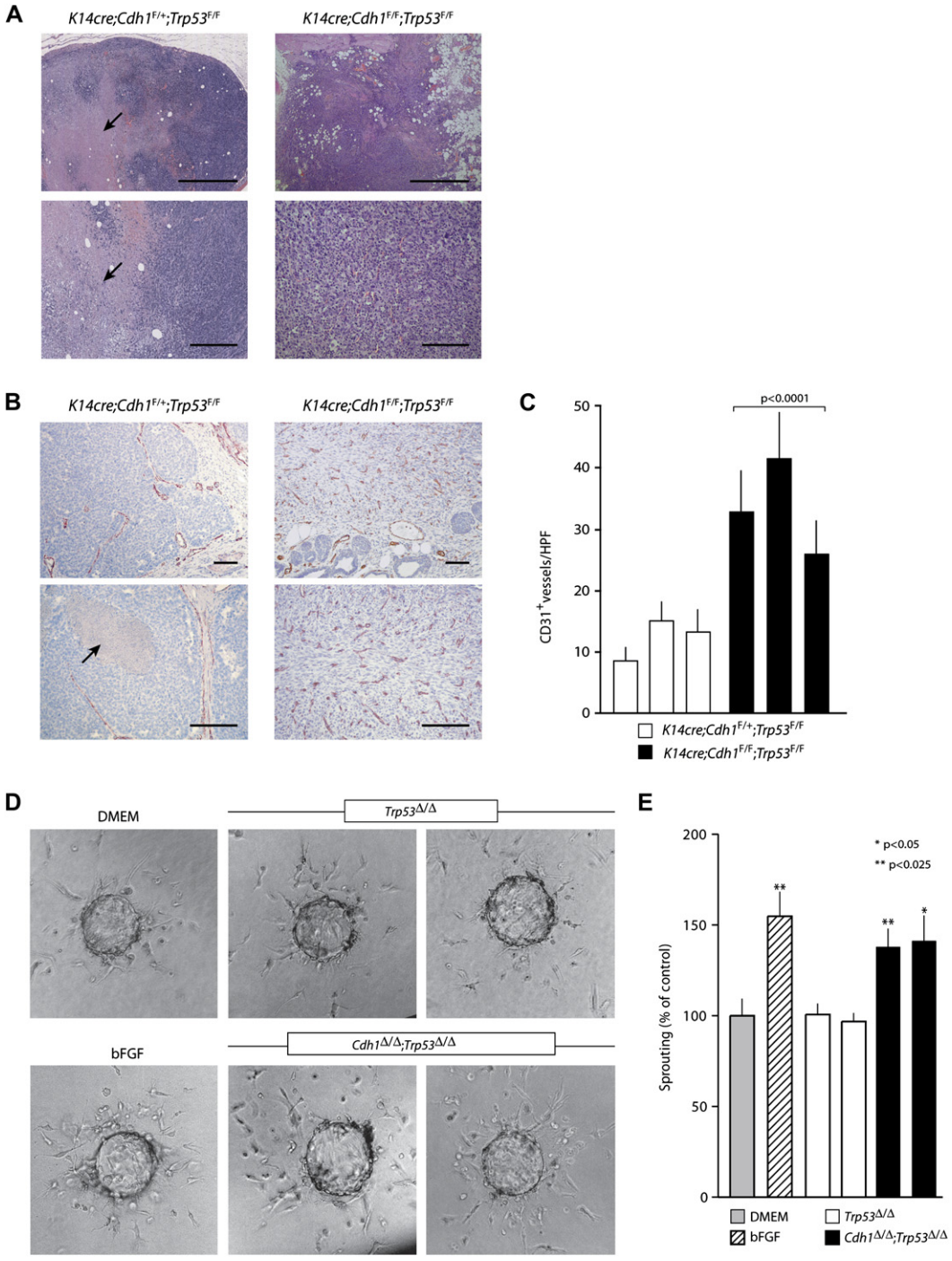

Figure 7. Induction of angiogenesis in murine ILC

A and B: Increased vascularization in vivo in mILC. **A:** H&E staining showing abundant necrosis (arrow) in *K14cre;Cdh1$^{F/+}$;Trp53$^{F/F}$* mammary tumors (left panels), whereas in *K14cre;Cdh1$^{F/+}$;Trp53$^{F/F}$* mILC (right panels) necrosis is absent. Bottom panels are a magnification of the upper panels. Scale bars, 1 mm (top panels) and 100 μm (bottom panels). **B:** Histopathology of *K14cre;Cdh1$^{F/+}$;Trp53$^{F/F}$* (left panel) and *K14cre;Cdh1$^{F/F}$;Trp53$^{F/F}$* (right panel) mammary tumors showing CD31 expression. Note the abundantly present CD31-positive vessels in mILC. Arrow indicates a necrotic area. Scale bars, 50 μm.

C: Quantification of the vascular density. The number of CD31-positive vessels were counted in ten low-power fields in tumors derived from three *K14cre;Cdh1$^{F/+}$;Trp53$^{F/F}$* females (white bars) and three *K14cre;Cdh1$^{F/F}$;Trp53$^{F/F}$* females (black bars). p values were calculated using ANOVA.

D and E: mILC induces in vitro angiogenesis. Bovine microvascular endothelial cells (BCEs) were cultured in a collagen matrix, after which serum-free CM from primary mammary tumors was added. Sprouting was induced more abundantly in the presence of conditioned medium (CM) from *Cdh1$^{\Delta/\Delta}$;Trp53$^{\Delta/\Delta}$* cells than in the presence of CM from *Trp53$^{\Delta/\Delta}$* cells. Sprouting shown in **D** was quantified in **E**. Error bars represent the standard deviation of triplicate measurements.

expression in *K14cre;Cdh1$^{F/F}$* females. We did, however, detect E-cadherin-negative epithelial in situ lesions in mammary glands from tumor-free *K14cre;Cdh1$^{F/F}$;Trp53$^{F/F}$* females. Loss of E-cadherin in this setting appears to be an early, tumor-initiating event, which is most likely tolerated because the apoptotic signals that are induced upon E-cadherin inactivation cannot be executed in the absence of functional p53.

Several biological programs have to be deregulated in order to transform normal cells into malignant, metastatic tumor cells (Hanahan and Weinberg, 2000). Loss of p53 results in loss of apoptotic responses and cell cycle control. This is, however, not sufficient to develop metastatic disease, as *K14cre;Trp53$^{F/F}$* and *K14cre;Cdh1$^{F/+}$;Trp53$^{F/F}$* females develop mammary carcinomas that only sporadically metastasize within the life span of the animals. Concomitant somatic loss of E-cadherin may provide key signals that promote tumor cell metastasis. First, mILC cells have acquired the potential to invade the surrounding stroma, which requires an increase in mobility and expression of the appropriate adhesion receptors. Second, the extremely dense and homogeneously distributed vascularization, as well as the capacity of mILC cells to function as a paracrine source of proangiogenic factors, indicate that somatic loss of E-cadherin may render mILC cells capable of inducing or enhancing angiogenesis. Finally, mILC cells have acquired anoikis resistance, which can facilitate tumor metastasis by permitting these cells to survive within the bloodstream and the lymphatic system and at distant organ sites. These findings imply that loss of E-cadherin invokes the capability to counteract the strong (p53-independent) proapoptotic signals that are induced upon loss of cell-matrix interactions. In summary, we conclude that, in our mILC model, loss of E-cadherin not only confers selective advantage during early stages of tumor development, but also promotes tumor progression and metastatic disease. Together, these findings support the notion that the signature of the primary tumor is a major determinant for clinical outcome (Van 't Veer et al., 2002). E-cadherin may thus represent a prime example of a tumor suppressor that fits the same-gene hypothesis, which states that certain mutations that provide a selective advantage during tumor initiation can also foster an invasive and metastatic phenotype (Hanahan and Weinberg, 2000; Bernards and Weinberg, 2002).

E-cadherin loss induces a phenotypic change from expansive adenocarcinoma to invasive lobular carcinoma

During mammary gland development, pluripotent cells can form both myoepithelial and luminal epithelial cell lineages. These cells, which express CK14, are thought to represent the mammary stem cells (Smalley and Ashworth, 2003; Althuis et al., 2005; Shackleton et al., 2006; Stingl et al., 2006). All mammary carcinomas from the *K14cre;Cdh1^{F};Trp53^{F}* model showed similar epithelial phenotypes, characterized by expression of the luminal marker CK8, occasional expression of the myoepithelial marker CK14, and absence of SMA and vimentin. However, the majority of *K14cre;Cdh1$^{F/F}$;Trp53$^{F/+}$* and *K14cre;Cdh1$^{F/F}$;Trp53$^{F/F}$* females developed invasive lobular instead of expansive carcinomas, indicating that the formation of mILC is a direct consequence of E-cadherin loss of function. E-cadherin is known to be important for both cell-cell adhesion and cell polarity (Drubin and Nelson, 1996), and it is therefore conceivable that loss of these functions may impair the duct-forming capacity of mammary epithelial cells. While the cell of origin remains elusive, our data are compatible with the notion that ductal and lobular carcinomas may originate from a common (CK14-positive) progenitor cell (Wellings et al., 1975; Wellings, 1980) and raise the possibility that the lobular carcinoma phenotype may directly result from loss of E-cadherin-mediated cell adhesion.

E-cadherin loss does not induce classical epithelial-to-mesenchymal transition

Numerous reports have shown that several transcription repressors of E-cadherin, such as SIP1, Snail, Slug, and Twist (Savagner et al., 1997; Batlle et al., 2000; Cano et al., 2000; Comijn et al., 2001; Hajra et al., 2002; Yang et al., 2004) can induce epithelial-to-mesenchymal transition (EMT) and subsequent metastasis. It has therefore been suggested that E-cadherin may be an important caretaker of the epithelial phenotype (Thiery, 2002). Our data show that E-cadherin loss alone is not sufficient for EMT, since all mILCs from our *K14cre;Cdh1$^{F/F}$;Trp53$^{F/F}$* model express the epithelial marker CK8 and lack expression of mesenchymal markers such as vimentin. Moreover, no significant difference in the incidence of carcinosarcomas was observed between *K14cre;Cdh1$^{F/+}$;Trp53$^{F/F}$* and *K14cre;Cdh1$^{F/F}$;Trp53$^{F/F}$* females (Table 1). While we cannot exclude the possibility that mILC cells transiently acquire mesenchymal properties during tumor invasion and dissemination, mILC might not require a complete EMT in order to metastasize. Conversely, the loss of E-cadherin-mediated cell adhesion and the spindle-shape morphology of mILC cells could be regarded as a partial EMT. It will therefore be important to determine whether tumor cell metastasis induced by expression of EMT regulators such as SIP1, Snail, Slug, and Twist is solely mediated through repression of E-cadherin, or whether other transcriptional targets contribute to this process.

ILC in mice and men

Mouse ILC recapitulates several key features of human ILC, including cellular morphology, absence of Her2/Neu/Erbb2 expression, invasive growth patterns, and sites of metastasis. Nevertheless, there are also differences between mILC and human ILC. One important discrepancy is that, in contrast to human ILC, mILCs do not express estrogen receptors. This difference is in line with the fact that, whereas most human breast cancers are ER positive, most established mouse models develop ER-negative mammary tumors (Nandi et al., 1995). Another potential difference between mILC and human ILC is the involvement of p53 mutations, which are thought to occur in a minority (4%–25%) of human ILC cases (Marchetti et al., 1993; Rosen et al., 1995; Soslow et al., 2000; Coradini et al., 2002; Arpino et al., 2004). Most analyses, however, have been performed using immunohistochemical detection of mutant p53 protein, leaving the possibility of functional p53 loss through alternative mechanisms. Supporting this are recent studies showing that 30%–40% of human lobular carcinomas have lost the *TP53* locus on chromosome 17p13 (Mohsin et al., 2005; Stange et al., 2006).

In summary, we have shown that somatic loss of E-cadherin and p53 in mice induces mammary tumors with histological characteristics similar to human ILC, a malignancy for which no mouse model was available until now. Concomitant loss of E-cadherin and p53 orchestrates a complex tactic that impacts on multiple aspects of oncogenesis, including tumor initiation,

angiogenesis, tumor cell survival, invasion, and metastasis. Our mILC model may prove a valuable tool for the identification of the molecular consequences of E-cadherin inactivation during mammary tumorigenesis and may facilitate designing and testing of treatment modalities for human ILC.

Experimental procedures

Construction of targeting vectors

To target the *Cdh1* locus, we isolated two clones from a mouse 129/Sv PAC library (RPCI-21, BACPAC Resources) using probes directed against exons 7 and 8 of *Cdh1*. From the PAC clones, 12 kb and 7.0 kb BamHI fragments were isolated using probes against *Cdh1* exons 4 and 14, respectively. The 5′ targeting construct was generated from the 12 kb BamHI fragment by inserting a *loxP*-PGK*neo*-*loxP* cassette into a unique AvrII site present in *Cdh1* intron 3. For the 3′ targeting construct, we used the 7 kb BamHI fragment to insert a *loxP*-PGK*hygro*-*loxP* cassette into a unique EcoRV site present in *Cdh1* intron 15.

Generation of *Cdh1*$^{F/+}$ conditional mice

A sequential gene targeting approach was undertaken to introduce single loxP sites in introns 3 and 15 of murine Cdh1 (Figures S1A–S1C). The 5′ and 3′ targeting constructs were released from the pGEM5 vector by NotI digestion. The 5′ targeting construct was electroporated into 129/Ola-derived E14-IB10 ES cells (Robanus-Maandag et al., 1998), and correctly targeted neomycin-resistant ES cells were identified by Southern blot analysis. One of these clones was subsequently electroporated with the 3′ targeting construct and subjected to hygromycin selection. Following identification of positive clones by Southern blot analysis, removal of the neomycin and hygromycin selection markers was achieved by transient Cre expression as described (Jonkers et al., 2001). Clones were analyzed by PCR using primers P1 (5′-ACATGTTTGTATCGATCTCAG-3′) and P2 (5′-CCATACACTGATAATGTCAGA-3′) to detect deletion of the neomycin cassette and primers P3 (5′-TCAATCTCAGAGCCCCACCTA-3′) and P4 (5′-CCTGCCATGATTGTCATGGAC-3′) to detect deletion of the hygromycin cassette, thus leaving behind single *loxP* sites in introns 3 and 15, respectively. Next, we confirmed dual targeting in *cis* by Southern blot analysis of SacI-digested DNA from positive ES cell clones with a *Chd1* exon 3 probe. The resulting *Cdh1*$^{F/+}$ ES cells were injected into C56Bl/6 blastocysts, and chimeras were crossed with FVB/N mice to produce heterozygous offspring. The resulting *Cdh1*$^{F/+}$ heterozygous and *Cdh1*$^{F/F}$ homozygous mice were viable and fertile and showed a normal life span, indicating that the *Cdh1*^{F} allele is fully functional. To test whether tissue-specific deletion of *Cdh1* exons 4 to 15 leads to functional inactivation of E-cadherin, we crossed *Cdh1*$^{F/F}$ homozygotes with *K14cre* transgenic mice, which express the Cre recombinase in several epithelial tissues, including skin and mammary epithelium (Jonkers et al., 2001). The resulting *K14cre;Cdh1*$^{F/F}$ animals showed stochastic loss of E-cadherin protein expression in skin epithelium, demonstrating that deletion of exons 4 to 15 of E-cadherin results in a functional null allele (Figure S1D). In contrast to the phenotypically normal *K14cre;Cdh1*$^{F/+}$ animals, *K14cre;Cdh1*$^{F/F}$ mice showed developmental defects in skin epithelium, resulting in disturbed hair follicle development, epidermal hyperplasia with frequent inflammation, progressive hair loss, and abnormal sebaceous gland development (data not shown). All animal experiments were approved by the Animal Ethical Committee and conducted in compliance with the Netherlands Cancer Institute and Dutch Animal Welfare guidelines.

DNA analysis

Genomic DNA was isolated from tissue by proteinase K lysis and organic extraction with phenol-chloroform. We performed Southern blot analysis using 10 μg of gDNA, digested with BglII or ScaI, to determine the status of the *Trp53* and *Cdh1*, respectively. Blotting and hybridization was performed as described (Jonkers et al., 2001). The *Trp53* probe has been described (Jonkers et al., 2001). The *Cdh1* probe was generated by PCR amplification of a 250 bp fragment of exon 16 using primers 5′-TTGAAGGATGCACCGGCCGGC-3′ and 5′-GGCGTGGTGGTGCCGGTGATG-3′. Probes were radiolabeled by PCR.

Genotyping of mutant mice

Detection of the *K14cre*, *Trp53*^{F}, and *Trp53*$^{\Delta}$ alleles was done as described previously (Jonkers et al., 2001). We detected the *Cdh1*^{F} allele by PCR amplification of the *loxP* site in intron 15, using primer pair P1 and P2, yielding 270 bp and 330 bp for the wild-type and floxed alleles, respectively. The deleted allele, *Cdh1*$^{\Delta}$, was detected by PCR using primers P1 and P4, yielding a product of 320 bp. PCR conditions were as described (Jonkers et al., 2001).

Antibodies

The following antibodies were used: (FITC-conjugated) mouse anti-E-cadherin (1:300; BD Biosciences), mouse anti-E-cadherin (1:1000; Zymed), rat anti-E-cadherin (DECMA-1; 1:2000) (Sigma), mouse anti-β-catenin (1:150; BD Biosciences), rat anti-cytokeratin (CK) 8 (Troma-1; 1:125; DSHB products), mouse anti-CK8 (CAM5.2; 1:400; BD Biosciences), rabbit anti-CK14 (1:10,000; BabCo), mouse anti-CK14 (1:200; Neomarkers), guinea pig anti-vimentin (1:400; RDI), mouse anti-vimentin (3B4; 1:400), mouse anti-SMA (1:10; Zymed), rabbit anti-SMA (1:350; Lab Vision), and goat anti-CD31 (1:200; Santa Cruz). Secondary antibodies were as follows: biotin-conjugated anti-mouse, anti-rat and anti-rabbit antibodies (DAKO), biotin-conjugated anti-guinea pig (Jackson ImmunoResearch), Alexa 568-conjugated anti-mouse (Molecular Probes), and RPE-conjugated anti-rat (Southern Biotechnology Associates).

Histological analysis

Tissues were isolated and fixed in 4% formaldehyde for 48 hr. Tissues were dehydrated, cut into 4 μm sections, and stained with hematoxylin and eosin. For single staining, fixed sections were rehydrated and incubated with primary antibodies. Endogenous peroxidases were blocked with 3% H_2O_2 and stained with biotin-conjugated secondary antibodies, followed by incubation with HRP-conjugated streptavidin-biotin complex (DAKO). Substrate was developed with either AEC or DAB (DAKO). For immunofluorescence, cells were grown on coverslips and fixed in ice-cold methanol. Cells were permeabilized using 0.5% Triton/PBS and subsequently incubated with primary antibodies. Then, cells were incubated with fluorochrome-conjugated secondary antibodies. DNA was stained with ToPro-3 (Molecular Probes), and cells were analyzed by confocal laser microscopy.

Cell culture

For the isolation of primary tumor cells, 50–100 mm^3 tumor sample was finely chopped using a McIlwain tissue chopper (The Mickle Laboratory Engineering Co.) and digested for 1 hr at 37°C in serum-free DMEM-F12 medium (Invitrogen Life Technologies) containing 0.1 mg/ml porcine pancreatic trypsin (Difco) and 0.2 mg/ml collagenase A (Roche). Cells were washed and fibroblasts were allowed to adhere for 1 hr at 37°C. Nonadherent epithelial cells were removed and cultured in DMEM-F12 medium containing 10% fetal bovine serum (FBS; ICN), 100 IU/ml penicillin, 100 μg/ml streptomycin, 5 ng/ml insulin, 5 ng/ml epidermal growth factor (EGF) (all Invitrogen Life Technologies), and 5 ng/ml cholera toxin (Sigma). 293T cells were cultured in Iscove's medium (Invitrogen Life Technologies) containing 10% FBS, 100 IU/ml penicillin, and 100 μg/ml streptomycin.

Retroviral production and transduction of cells

The mouse E-cadherin cDNA (a kind gift from Dr. G. Christofori, University of Basel, Switzerland) was subcloned into pBABE-puro and pMSCV-blast retroviral vectors. For production of ecotropic retroviruses, 10^6 Phoenix packaging cells were seeded onto 10 cm petri dishes and transiently transfected after 24 hr with either pBABE-*Cdh1* or pMSCV-*Cdh1* using Fugene-6 transfection reagent (Roche). Supernatant containing viral particles was harvested after 72 hr and passed through a 45 μm filter. Retroviral infection of tumor cells was performed three times for 4 hr in the presence of 4 μg/ml polybrene (Sigma). Lentiviral particles were produced by seeding 10^6 293T cells onto a 10 cm petri dish and transient transfection after 24 hr with third-generation packaging constructs (Dull et al., 1998) and a luciferase-encoding transfer vector (LV-luc). The LV-luc vector was constructed by replacing the GFP coding region from pCSCG (Miyoshi et al., 1998) with the luciferase coding sequence from pNF-κB-Luc (Clontech). Supernatant containing lentiviral particles was harvested after 48 and 72 hr, passed through a 45 μm filter, and concentrated by centrifugation at 20,000 rpm for 2.5 hr. Virus particles were dissolved in serum-free DMEM-F12 (Invitrogen), snap frozen in liquid

nitrogen, and stored at −80°C. Tumor cells were infected with LV-luc for 16 hr in the presence of 4 μg/ml polybrene.

Orthotopic transplantations and bioluminescence imaging

Three-week-old *Rag2*$^{-/-}$*;IL2R*γ*c*$^{-/-}$ BALB/c females (Gimeno et al., 2004) were anesthetized by intraperitoneal (i.p.) injection of a mixture containing 25 μl hypnorm (Janssen Pharmaceutica), 25 μl dormicum (Roche), and 50 μl water. The fourth mammary gland was exposed, and endogenous mammary epithelial tissue was removed. Next, approximately 10,000 luciferase-transduced tumor cells were injected in the cleared fat pad using a Hamilton syringe, after which the animals were sutured. After a recovery period of 2 weeks, mice were anesthetized with isofluorane (Janssen Pharmaceutica), injected i.p. with 225 μg/g body weight *n*-luciferin (potassium salt; Xenogen Corp.), and imaged on a IVIS-100 bioluminescence imager (Xenogen Corp.).

Anoikis assay

Cells were plated at a density of 75,000 cells per well in a 6-well ultra-low cluster polystyrene culture dish (Corning). After the indicated time interval, cells were harvested and incubated at 37°C with 0.25% trypsin (Invitrogen) for 1 min to prevent cell aggregation. FITC-conjugated Annexin-V (IQ Products) and ToPro-3 (Molecular Probes), were added and Annexin-V-positive apoptotic cells were analyzed by FACS as described (Derksen et al., 2003). Statistical significance was calculated using the Student's t test.

Sprouting assay

Bovine microvascular endothelial cells (BCEs), kindly provided by Dr. M. Furie (State University of New York, Stony Brook, NY), were cultured on gelatin-coated flasks in DMEM supplemented with 10% FBS (Perbio Science), 50 IU/ml penicillin, 50 ng/ml streptomycin, and 30 μg/ml endothelial cell growth supplement (ECGS; BD Biosciences). BCEs were mixed with gelatin-coated cytodex-3 beads (Sigma) at a concentration of 100 cells per bead and cultured for 72 hr in BCE medium supplemented with 25% serum-free conditioned medium from *Trp53*$^{\Delta/\Delta}$ or *Cdh1*$^{\Delta/\Delta}$*;Trp53*$^{\Delta/\Delta}$ mILC cells. The beads were subsequently resuspended at a concentration of 25 beads per 100 μl in a collagen gel mixture consisting of 2.4 mg/ml vitrogen-100 (Collagen, Fremont, CA), 1× α-MEM (Life Technologies), and 1.2 mg/ml sodium bicarbonate (Merck). Solidified gel was overlaid with BCE medium supplemented with serum-free 25% conditioned medium from the indicated cell lines, 20 ng/ml bFGF (Reliatech), or DMEM as control. Photographs were taken after 48 hr. Five concentric rings were projected over the photographs, and the number of intersections of rings and sprouting endothelial cells was determined and used as a measure of in vitro tube formation. Statistical analyses were done using the Student's t test.

Supplemental data

The Supplemental Data include three supplemental figures and one supplemental table and can be found with this article online at http://www.cancercell.org/cgi/content/full/10/5/437/DC1/.

Acknowledgments

We wish to thank Gerhard Christofori for the mouse E-cadherin cDNA; Daniel Silver for lentiviral packaging vectors; Annette Dirac for providing the lentiviral luciferase transfer vector; Eline van der Burg for excellent technical support; Lauran Oomen for help with confocal microscopy; and Daniel Peeper, Arnoud Sonnenberg, and Hein te Riele for critically reading the manuscript. Members of the Jonkers, Agami, and Peeper labs are acknowledged for reagents, help, and fruitful discussions. We are also indebted to the animal facility and the animal pathology lab. This work was supported by grants from the Netherlands Organization for Scientific Research (NWO-Vidi 917.36.347) and the Dutch Cancer Society (NKI 2002-2635). P.W.B.D. is supported by a grant from the Netherlands Organization for Scientific Research (NWO-Veni 916.56.135).

Received: March 27, 2006
Revised: June 1, 2006
Accepted: September 15, 2006
Published: November 13, 2006

References

Adams, D.J., and Bradley, A. (2002). Induced mitotic recombination: A switch in time. Nat. Genet. *30*, 6–7.

Althuis, M.D., Dozier, J.M., Anderson, W.F., Devesa, S.S., and Brinton, L.A. (2005). Global trends in breast cancer incidence and mortality 1973–1997. Int. J. Epidemiol. *34*, 405–412.

Arpino, G., Bardou, V.J., Clark, G.M., and Elledge, R.M. (2004). Infiltrating lobular carcinoma of the breast: Tumor characteristics and clinical outcome. Breast Cancer Res. *6*, R149–R156.

Batlle, E., Sancho, E., Franci, C., Dominguez, D., Monfar, M., Baulida, J., and Garcia De Herreros, A. (2000). The transcription factor snail is a repressor of E-cadherin gene expression in epithelial tumour cells. Nat. Cell Biol. *2*, 84–89.

Bernards, R., and Weinberg, R.A. (2002). A progression puzzle. Nature *418*, 823.

Berx, G., and van Roy, F. (2001). The E-cadherin/catenin complex: An important gatekeeper in breast cancer tumorigenesis and malignant progression. Breast Cancer Res. *3*, 289–293.

Berx, G., Cleton-Jansen, A.M., Nollet, F., de Leeuw, W.J., van de Vijver, M., Cornelisse, C., and van Roy, F. (1995). E-cadherin is a tumour/invasion suppressor gene mutated in human lobular breast cancers. EMBO J. *14*, 6107–6115.

Berx, G., Becker, K.F., Hofler, H., and van Roy, F. (1998). Mutations of the human E-cadherin (CDH1) gene. Hum. Mutat. *12*, 226–237.

Boussadia, O., Kutsch, S., Hierholzer, A., Delmas, V., and Kemler, R. (2002). E-cadherin is a survival factor for the lactating mouse mammary gland. Mech. Dev. *115*, 53–62.

Cano, A., Perez-Moreno, M.A., Rodrigo, I., Locascio, A., Blanco, M.J., del Barrio, M.G., Portillo, F., and Nieto, M.A. (2000). The transcription factor snail controls epithelial-mesenchymal transitions by repressing E-cadherin expression. Nat. Cell Biol. *2*, 76–83.

Cavallaro, U., and Christofori, G. (2004). Cell adhesion and signalling by cadherins and Ig-CAMs in cancer. Nat. Rev. Cancer *4*, 118–132.

Cleton-Jansen, A.M., Moerland, E.W., Kuipers-Dijkshoorn, N.J., Callen, D.F., Sutherland, G.R., Hansen, B., Devilee, P., and Cornelisse, C.J. (1994). At least two different regions are involved in allelic imbalance on chromosome arm 16q in breast cancer. Genes Chromosomes Cancer *9*, 101–107.

Comijn, J., Berx, G., Vermassen, P., Verschueren, K., van Grunsven, L., Bruyneel, E., Mareel, M., Huylebroeck, D., and van Roy, F. (2001). The two-handed E box binding zinc finger protein SIP1 downregulates E-cadherin and induces invasion. Mol. Cell *7*, 1267–1278.

Conacci-Sorrell, M., Zhurinsky, J., and Ben Ze'ev, A. (2002). The cadherin-catenin adhesion system in signaling and cancer. J. Clin. Invest. *109*, 987–991.

Coradini, D., Pellizzaro, C., Veneroni, S., Ventura, L., and Daidone, M.G. (2002). Infiltrating ductal and lobular breast carcinomas are characterised by different interrelationships among markers related to angiogenesis and hormone dependence. Br. J. Cancer *87*, 1105–1111.

Derksen, P.W., de Gorter, D.J., Meijer, H.P., Bende, R.J., van Dijk, M., Lokhorst, H.M., Bloem, A.C., Spaargaren, M., and Pals, S.T. (2003). The hepatocyte growth factor/Met pathway controls proliferation and apoptosis in multiple myeloma. Leukemia *17*, 764–774.

Drubin, D.G., and Nelson, W.J. (1996). Origins of cell polarity. Cell *84*, 335–344.

Dull, T., Zufferey, R., Kelly, M., Mandel, R.J., Nguyen, M., Trono, D., and Naldini, L. (1998). A third-generation lentivirus vector with a conditional packaging system. J. Virol. *72*, 8463–8471.

Frixen, U.H., Behrens, J., Sachs, M., Eberle, G., Voss, B., Warda, A., Lochner, D., and Birchmeier, W. (1991). E-cadherin-mediated cell-cell adhesion prevents invasiveness of human carcinoma cells. J. Cell Biol. *113*, 173–185.

Fujita, N., Jaye, D.L., Kajita, M., Geigerman, C., Moreno, C.S., and Wade, P.A. (2003). MTA3, a Mi-2/NuRD complex subunit, regulates an invasive growth pathway in breast cancer. Cell *113*, 207–219.

Gimeno, R., Weijer, K., Voordouw, A., Uittenbogaart, C.H., Legrand, N., Alves, N.L., Wijnands, E., Blom, B., and Spits, H. (2004). Monitoring the effect of gene silencing by RNA interference in human $CD34^+$ cells injected into newborn $RAG2^{-/-}$ $\gamma c^{-/-}$ mice: Functional inactivation of p53 in developing T cells. Blood *104*, 3886–3893.

Graff, J.R., Herman, J.G., Lapidus, R.G., Chopra, H., Xu, R., Jarrard, D.F., Isaacs, W.B., Pitha, P.M., Davidson, N.E., and Baylin, S.B. (1995). E-cadherin expression is silenced by DNA hypermethylation in human breast and prostate carcinomas. Cancer Res. *55*, 5195–5199.

Hajra, K.M., Chen, D.Y., and Fearon, E.R. (2002). The SLUG zinc-finger protein represses E-cadherin in breast cancer. Cancer Res. *62*, 1613–1618.

Hanahan, D., and Weinberg, R.A. (2000). The hallmarks of cancer. Cell *100*, 57–70.

Hulsken, J., Birchmeier, W., and Behrens, J. (1994). E-cadherin and APC compete for the interaction with beta-catenin and the cytoskeleton. J. Cell Biol. *127*, 2061–2069.

Jonkers, J., Meuwissen, R., Van Der Gulden, H., Peterse, H., van der Valk, M., and Berns, A. (2001). Synergistic tumor suppressor activity of BRCA2 and p53 in a conditional mouse model for breast cancer. Nat. Genet. *29*, 418–425.

Korkola, J.E., DeVries, S., Fridlyand, J., Hwang, E.S., Estep, A.L., Chen, Y.Y., Chew, K.L., Dairkee, S.H., Jensen, R.M., and Waldman, F.M. (2003). Differentiation of lobular versus ductal breast carcinomas by expression microarray analysis. Cancer Res. *63*, 7167–7175.

Lehr, H.A., Folpe, A., Yaziji, H., Kommoss, F., and Gown, A.M. (2000). Cytokeratin 8 immunostaining pattern and E-cadherin expression distinguish lobular from ductal breast carcinoma. Am. J. Clin. Pathol. *114*, 190–196.

Marchetti, A., Buttitta, F., Pellegrini, S., Campani, D., Diella, F., Cecchetti, D., Callahan, R., and Bistocchi, M. (1993). p53 mutations and histological type of invasive breast carcinoma. Cancer Res. *53*, 4665–4669.

Miyoshi, H., Blomer, U., Takahashi, M., Gage, F.H., and Verma, I.M. (1998). Development of a self-inactivating lentivirus vector. J. Virol. *72*, 8150–8157.

Mohsin, S.K., O'Connell, P., Allred, D.C., and Libby, A.L. (2005). Biomarker profile and genetic abnormalities in lobular carcinoma in situ. Breast Cancer Res. Treat. *90*, 249–256.

Moody, S.E., Perez, D., Pan, T.C., Sarkisian, C.J., Portocarrero, C.P., Sterner, C.J., Notorfrancesco, K.L., Cardiff, R.D., and Chodosh, L.A. (2005). The transcriptional repressor Snail promotes mammary tumor recurrence. Cancer Cell *8*, 197–209.

Nandi, S., Guzman, R.C., and Yang, J. (1995). Hormones and mammary carcinogenesis in mice, rats, and humans: A unifying hypothesis. Proc. Natl. Acad. Sci. USA *92*, 3650–3657.

Oda, T., Kanai, Y., Oyama, T., Yoshiura, K., Shimoyama, Y., Birchmeier, W., Sugimura, T., and Hirohashi, S. (1994). E-cadherin gene mutations in human gastric carcinoma cell lines. Proc. Natl. Acad. Sci. USA *91*, 1858–1862.

Perez-Moreno, M., Jamora, C., and Fuchs, E. (2003). Sticky business: Orchestrating cellular signals at adherens junctions. Cell *112*, 535–548.

Perl, A.K., Wilgenbus, P., Dahl, U., Semb, H., and Christofori, G. (1998). A causal role for E-cadherin in the transition from adenoma to carcinoma. Nature *392*, 190–193.

Robanus-Maandag, E., Dekker, M., van der Valk, M., Carrozza, M.L., Jeanny, J.C., Dannenberg, J.H., Berns, A., and te Riele, H. (1998). p107 is a suppressor of retinoblastoma development in pRb-deficient mice. Genes Dev. *12*, 1599–1609.

Rosen, P.P., Lesser, M.L., Arroyo, C.D., Cranor, M., Borgen, P., and Norton, L. (1995). p53 in node-negative breast carcinoma: An immunohistochemical study of epidemiologic risk factors, histologic features, and prognosis. J. Clin. Oncol. *13*, 821–830.

Savagner, P., Yamada, K.M., and Thiery, J.P. (1997). The zinc-finger protein slug causes desmosome dissociation, an initial and necessary step for growth factor-induced epithelial-mesenchymal transition. J. Cell Biol. *137*, 1403–1419.

Shackleton, M., Vaillant, F., Simpson, K.J., Stingl, J., Smyth, G.K., Asselin-Labat, M.L., Wu, L., Lindeman, G.J., and Visvader, J.E. (2006). Generation of a functional mammary gland from a single stem cell. Nature *439*, 84–88.

Simpson, P.T., Gale, T., Fulford, L.G., Reis-Filho, J.S., and Lakhani, S.R. (2003). The diagnosis and management of pre-invasive breast disease: Pathology of atypical lobular hyperplasia and lobular carcinoma in situ. Breast Cancer Res. *5*, 258–262.

Smalley, M., and Ashworth, A. (2003). Stem cells and breast cancer: A field in transit. Nat. Rev. Cancer *3*, 832–844.

Soslow, R.A., Carlson, D.L., Horenstein, M.G., and Osborne, M.P. (2000). A comparison of cell cycle markers in well-differentiated lobular and ductal carcinomas. Breast Cancer Res. Treat. *61*, 161–170.

Stange, D.E., Radlwimmer, B., Schubert, F., Traub, F., Pich, A., Toedt, G., Mendrzyk, F., Lehmann, U., Eils, R., Kreipe, H., and Lichter, P. (2006). High-resolution genomic profiling reveals association of chromosomal aberrations on 1q and 16p with histologic and genetic subgroups of invasive breast cancer. Clin. Cancer Res. *12*, 345–352.

Stingl, J., Eirew, P., Ricketson, I., Shackleton, M., Vaillant, F., Choi, D., Li, H.I., and Eaves, C.J. (2006). Purification and unique properties of mammary epithelial stem cells. Nature *439*, 993–997.

Takeichi, M. (1995). Morphogenetic roles of classic cadherins. Curr. Opin. Cell Biol. *7*, 619–627.

Thiery, J.P. (2002). Epithelial-mesenchymal transitions in tumour progression. Nat. Rev. Cancer *2*, 442–454.

Tinkle, C.L., Lechler, T., Pasolli, H.A., and Fuchs, E. (2004). Conditional targeting of E-cadherin in skin: Insights into hyperproliferative and degenerative responses. Proc. Natl. Acad. Sci. USA *101*, 552–557.

Tunggal, J.A., Helfrich, I., Schmitz, A., Schwarz, H., Gunzel, D., Fromm, M., Kemler, R., Krieg, T., and Niessen, C.M. (2005). E-cadherin is essential for in vivo epidermal barrier function by regulating tight junctions. EMBO J. *24*, 1146–1156.

Van 't Veer, L.J., Dai, H., van de Vijver, M.J., He, Y.D., Hart, A.A., Mao, M., Peterse, H.L., van der Kooy, K., Marton, M.J., Witteveen, A.T., et al. (2002). Gene expression profiling predicts clinical outcome of breast cancer. Nature *415*, 530–536.

Vleminckx, K., Vakaet, L., Jr., Mareel, M., Fiers, W., and van Roy, F. (1991). Genetic manipulation of E-cadherin expression by epithelial tumor cells reveals an invasion suppressor role. Cell *66*, 107–119.

Vos, C.B., Cleton-Jansen, A.M., Berx, G., de Leeuw, W.J., ter Haar, N.T., van Roy, F., Cornelisse, C.J., Peterse, J.L., and van de Vijver, M.J. (1997). E-cadherin inactivation in lobular carcinoma in situ of the breast: An early event in tumorigenesis. Br. J. Cancer *76*, 1131–1133.

Wellings, S.R. (1980). Development of human breast cancer. Adv. Cancer Res. *31*, 287–314.

Wellings, S.R., Jensen, H.M., and Marcum, R.G. (1975). An atlas of subgross pathology of the human breast with special reference to possible precancerous lesions. J. Natl. Cancer Inst. *55*, 231–273.

Yang, J., Mani, S.A., Donaher, J.L., Ramaswamy, S., Itzykson, R.A., Come, C., Savagner, P., Gitelman, I., Richardson, A., and Weinberg, R.A. (2004). Twist, a master regulator of morphogenesis, plays an essential role in tumor metastasis. Cell *117*, 927–939.

Yoshiura, K., Kanai, Y., Ochiai, A., Shimoyama, Y., Sugimura, T., and Hirohashi, S. (1995). Silencing of the E-cadherin invasion-suppressor gene by CpG methylation in human carcinomas. Proc. Natl. Acad. Sci. USA *92*, 7416–7419.

Young, P., Boussadia, O., Halfter, H., Grose, R., Berger, P., Leone, D.P., Robenek, H., Charnay, P., Kemler, R., and Suter, U. (2003). E-cadherin controls adherens junctions in the epidermis and the renewal of hair follicles. EMBO J. *22*, 5723–5733.

Zhao, H., Langerod, A., Ji, Y., Nowels, K.W., Nesland, J.M., Tibshirani, R., Bukholm, I.K., Karesen, R., Botstein, D., Borresen-Dale, A.L., and Jeffrey, S.S. (2004). Different gene expression patterns in invasive lobular and ductal carcinomas of the breast. Mol. Biol. Cell *15*, 2523–2536.